

On Touching Triangle Graphs

Emden R. Gansner¹, Yifan Hu¹, and Stephen G. Kobourov²

¹ AT&T Labs - Research, Florham Park, NJ

{erg, yifanhu}@research.att.com

² University of Arizona, Tucson, AZ

kobourov@cs.arizona.edu

Abstract. In this paper, we consider the problem of representing graphs by triangles whose sides touch. As a simple necessary condition, we show that pairs of vertices must have a small common neighborhood. On the positive side, we present linear time algorithms for creating touching triangle representations for outerplanar graphs, square grid graphs, and hexagonal grid graphs. We note that this class of graphs is not closed under minors, making characterization difficult. However, we present a complete characterization of the subclass of biconnected graphs that can be represented as triangulations of some polygon.

1 Introduction

Planar graphs are a widely studied class of graphs that includes naturally occurring subclasses such as trees and outerplanar graphs. Typically planar graphs are drawn using the node-link model, where vertices are represented by a point and edges are represented by line segments. Alternative representations, such as contact circles [2] and contact triangles [7] have also been explored. In these representations, a vertex is a circle or triangle, and an edge is represented by pairwise contact at a common point.

In this paper, we explore the case where vertices are polygons, with an edge whenever the sides of two polygons touch. Specifically, given a planar graph $G = (V, E)$, we would like to find a set of polygons R such that:

1. there is bijection between V and R ;
2. two polygons touch non-trivially if and only if the corresponding vertices are adjacent in G ;
3. and each polygon is convex.

Note that, unlike the case of contact circle and contact triangle representations, two polygons that share a common point are not considered adjacent. It is easy to see that all planar graphs have representations meeting conditions 1 and 2 above, as pointed out by de Fraysseix *et al.* [6]. Starting with a straight-line planar drawing of G , a polygon for each vertex can be defined by taking the midpoints of all adjacent edges and the centers of all neighboring faces. The *complexity*, i.e., number of its sides, of the resulting polygons can be as high as $|V| - 1$, as it is proportional to the degree of the corresponding vertex. Moreover, the polygons would not necessarily be convex.

A theorem of Thomassen [19] implies that all planar graphs can be represented using convex hexagons. (This also follows from results by Kant [14] and de Fraysseix *et al.* [6].) Gansner *et al.* [9] have shown that six sides are also necessary. This leads us to consider which planar graphs can be represented by polygons with fewer than six sides.

This paper presents some initial results for the case of touching triangles. We assume we are dealing with connected planar graphs $G = (V, E)$. We let TTG denote the class of graphs that have a touching triangle representation. In Section 2, we show that all outerplanar graphs are in TTG . Similarly, we show in Section 3 that all subgraphs of a square or hexagonal grid are in TTG . All of these representations can be computed in linear time. Section 4 characterizes the special

case of graphs arising from triangulations of simple, hole-less polygons. Finally, in Section 5, we show that, for graphs in TTG , pairs of vertices have very limited common neighborhoods. This allows us to identify concrete examples of graphs not in TTG .

1.1 Related Work

Results on representing planar graphs as “contact systems” can be dated back to Koebe’s 1936 theorem [15] which states that any planar graph can be represented as a contact graph of disks in the plane. When the regions are further restricted to rectangles, not all planar graph can be represented. Rahman *et al.* [17] describe a linear time algorithm for constructing rectangular contact graphs, if one exists. Buchsbaum *et al.* [3] provide a characterization of the class of graphs that admit rectangular contact graph representation. The version of the problem where it is further required that there are no holes in the rectangular contact graph representation is known as the rectangular dual problem. He [11] describes a linear time algorithm for constructing a rectangular dual of a planar graph, if one exists. Kant’s linear time algorithm for drawing degree-3 planar graphs on a hexagonal grid [14] can be used to obtain hexagonal drawings for planar graphs.

In VLSI floor-planning it is often required to partition a rectangle into rectilinear regions so that non-trivial region adjacencies correspond to a given planar graph. It is natural to try to minimize the complexities of the resulting regions and the best known results are due to He [12] and Liao *et al.* [16] who show that regions need not have more than 8 sides. Both of these algorithms run in $O(n)$ time and produce layouts on an integer grid of size $O(n) \times O(n)$, where n is the number of vertices.

Rectilinear cartograms can be defined as rectilinear contact graphs for vertex weighted planar graphs, where the area of a rectilinear region must be proportional to the weight of its corresponding node. Even with this extra condition, de Berg *et al.* [4] show that rectilinear cartograms with constant region complexity can be constructed in $O(n \log n)$ time. Specifically, a rectilinear cartogram with region complexity 40 can always be found.

2 Outerplanar Graphs

In this section, we show that any outerplanar graph can be represented by a set of touching triangles, that is, outerplanar graphs belong to the class TTG . Here we assume that we are given an outerplanar graph $G = (V, E)$ and the goal is to represent G as a set of touching triangles. We describe a linear time algorithm based on inserting the vertices of G in an easy-to-compute “peeling” order. Figure 1 illustrates the algorithm with an example.

2.1 Algorithm Overview

1. Compute an outerplanar embedding of G .
2. Compute a reverse “peeling” order of the vertices of G .
3. Insert region(s) corresponding to the current set of vertices in the peeling order, while maintaining a concave upper envelope.

We now look at each step in more detail. The first step of the algorithm is to compute an outerplanar embedding of the graph, that is, an embedding in which all the vertices are on the outer face. For a given planar graph $G = (V, E)$, this can be easily done in linear time as follows. Let w be a new vertex and let $G' = (V', E')$, where $V' = V \cup \{w\}$ and $E' = E \cup \{(v, w) \text{ for all } v \in V\}$. Note that G' is planar: if it contained a subgraph homeomorphic to K_5 or $K_{3,3}$, then

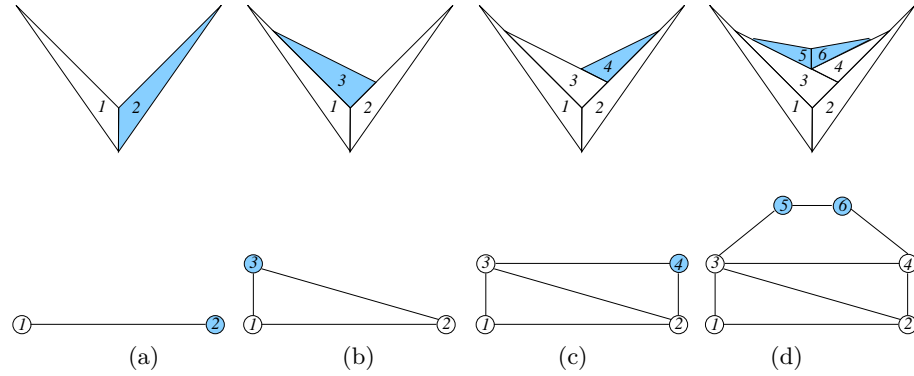


Fig. 1. Incremental construction of the TTG representation of an outerplanar graph on 6 vertices. The shaded vertices on the bottom row and shaded regions on the top row are the ones processed at the current step. Note that the upper envelope on the top row forms a concave chain at all times.

G would contain a subgraph homeomorphic to K_4 or $K_{3,2}$, which would imply that G was not outerplanar to begin with as these are forbidden graphs for outerplanar graphs (Theorem 11.10, [10]). We can then compute a planar embedding for G' with w on the outer face. Removing w and all its edges yields the desired outerplanar embedding.

The second step of the algorithm is to compute a reverse “peeling” order of the vertices of G . Such an order is defined by peeling off one face at a time and keeping track of the set of removed vertices. Note that, as G is outerplanar, each such set is a path with one or more vertices and only its endpoints are connected to the rest of the graph. Moreover, as the dual of an outerplanar graph is a tree, any pair of adjacent faces shares exactly one edge. As a result of this step in the algorithm, all the vertices of G are partitioned into disjoint sets with increasing labels. Since the order is reversed, the last face peeled is the one with vertices v_1, v_2, v_3 .

The third step of the algorithm is to create the touching triangles representation of G , by processing the graph using the peeling order from the second step. We begin by placing the vertices in the last peeled face. Suppose the last peeled face has exactly 3 vertices, v_1, v_2, v_3 . Without loss of generality, let the edge (v_2, v_3) separate this face from the rest of the graph. We create two triangles corresponding to v_1 and v_2 and place these triangles so that they have one adjacent side and two other sides of the triangles create a concave upper envelope; see Fig. 1(a). The third vertex, v_3 , corresponds to a triangle that can be placed in the created concavity so that it has one side touching the triangle that corresponds to v_1 and another side touching the triangle that corresponds to v_2 . The size of the triangle is computed so that the upper envelope is still concave and contains a side of each of the three triangles; see Fig. 1(b). Taking the midpoints of the adjacent sides of the already placed triangles for v_1 and v_2 would do.

In general, when processing the current set of one or more vertices in the peeling order, they are of the form $v_k, v_{k+1}, \dots, v_{k+j}$, $j \geq 0$. These vertices form a path in G and $v_{k+1}, \dots, v_{k+j-1}$ each have degree 2 in the current graph, that is, they are not connected to any other vertices of the graph processed so far, due to outerplanarity. Furthermore, v_k and v_{k+j} are connected to two other vertices in G which have already been processed; call them v_l and v_r . Due to outerplanarity, v_l and v_r correspond to two adjacent triangles in the concave upper envelope. If $j = 0$, we just need to create one triangle that corresponds to the single current vertex v_k and place it so that it is adjacent to the already processed triangles corresponding to v_l and v_r , and ensuring that the new triangle preserves the concavity of the upper envelope. Once again, taking the midpoints of the adjacent sides of the already placed triangles for v_l and v_r suffices; see Fig. 1(c).

If $j > 0$, then we represent the $j+1$ current vertices as a “fan” of triangles that have adjacent sides and are also adjacent to the two already placed triangles that correspond to v_l and v_r .

Finally, we ensure that the upper envelope of the resulting group of triangles forms a concave envelope; see Figure 1(d). Note that this idea can be applied to the case when the first peeled face is made of more than 3 vertices.

The algorithm maintains the following two invariants:

1. the upper envelope of the touching-triangles representation is concave.
2. all vertices that might still have incoming edges in a future stage of the algorithm have an exposed side in their corresponding triangle on the upper envelope.

The first step of this algorithm can be done in linear time as it is a slight modification of a standard planar embedding algorithm such as that by Hopcroft and Tarjan [13]. The second step can also be done in linear time as computing the “peeling ordering” requires constant time per face, given the embedding of the graph from the previous step. In the third step, we record the three edges of each triangle corresponding to each processed vertex. Inserting a new chain of vertices involves finding the midpoint of the exposed edges, and forming the “fan” of new triangles, all tasks which require constant time per vertex and add up to linear overall time. Thus, we have the following theorem:

Theorem 1. *A touching triangles representation can be computed in linear time for any outerplanar graph.*

3 Grid Graphs

In this section, we show that any subgraph of a square or hexagonal grid graph can be represented by a set of touching triangles. We describe a linear time algorithm based on inserting the vertices of the graph in an outward fashion starting from an interior square/hexagon. We illustrate the algorithm with examples in Figure 2.

3.1 Algorithm Overview

We first consider *TTG* representations for grid graphs.

1. Compute a planar embedding of G .
2. Compute a “spiral” order of the vertices of G .
3. Insert region(s), corresponding to a vertex or a path of vertices in the spiral order, while maintaining a concave upper envelope in each quadrant (in the case of square grid), or by carving out triangles out of trapezoids that correspond to the current spiral segment (in the case of hexagonal grid).

The first step of the algorithm is to compute a planar embedding of the graph, which can be done in linear time [13]. Next we compute a “spiral” order of the vertices. Such an order is defined by a Hamiltonian path which starts with the innermost face and visits all the vertices as shown in Fig. 2. Note that this is well defined for symmetric grid graphs but can be modified to handle asymmetric grid graphs and subgraphs of grid graphs.

In the case of square grids, the plane is partitioned into four quadrants and in each quadrant the spiral order introduces vertices in paths of increasing lengths $(1, 3, 5, \dots)$. In general these paths can be introduced recursively, provided that the upper envelope of the quadrant remains concave. The insertion of regions is similar to the process described for outerplanar graphs above.

In the case of hexagonal grids the plane is partitioned into six sectors and in each sector the spiral order introduces vertices in paths of increasing lengths $(1, 3, 5, \dots)$. In general, these paths can be introduced directly by adding an adjacent trapezoidal region and carving it into triangles.

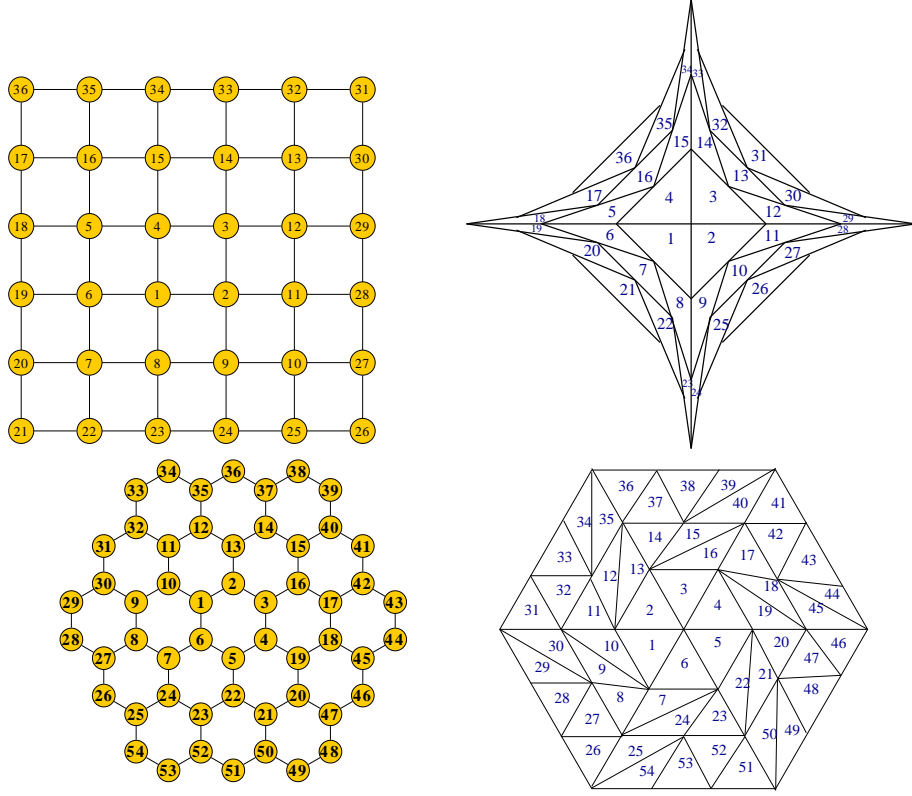


Fig. 2. Grid graphs (left) as touching triangles (right). The Hamiltonian path that visits all the vertices in the spiral order is given by the labels of the vertices.

The above algorithms show how to construct a *TTG* representation for any square or hexagonal grid graph. To get a *TTG* representation for any subgraph, one need only remove the triangles corresponding to vertices unused in the subgraph, and adjust the remaining triangles to remove any contacts corresponding to unused edges. Thus, we have the following theorem:

Theorem 2. *A touching triangles representation can be computed in linear time for any subgraph of a square or hexagonal grid graph.*

4 Triangulations

If we require each face in a triangle representation to have exactly three vertices, i.e., the vertex of one triangle cannot touch the side of another, we get the special case of *TTGs* we call *triangulation graphs*. These representations clearly correspond to creating a triangular mesh [1, 5], allowing Steiner points, within the interior of a polygon. For example, the representation in the bottom right of Fig. 2 is a triangulation graph and the representation in the top right of Fig. 2 is not.

It is easy to see that triangulation graphs form a strict subset of *TTGs*. For example, K_4 is a *TTG* but not a triangulation graph. It is also immediate that a triangulation graph has maximum degree 3, because by the definition of triangulation graphs, the vertex of one triangle cannot touch the side of another.

Lemma 1. *If G is a triangulation graph with no nodes of degree 1, G has at least 3 nodes of degree 2.*

Proof: The only triangles that can contribute to the polygon's boundary or outer face must have degree 2 in the graph, each contributing exactly 1 edge to the boundary. Since the polygon has at least 3 edges, the result follows. \square

A further subclass consists of the *filled triangulation graphs*, those who have a representation whose corresponding polygon is simple with no holes. It is possible to fully characterize the biconnected subset of these graphs.

Theorem 3. *Assume G is biconnected. G is a filled triangulation graph if and only if G has:*

1. *only nodes of degree 2 or 3*
2. *an embedding in the plane such that:*
 - (a) *every internal node has degree 3;*
 - (b) *there are at least 3 nodes of degree 2 on the boundary;*
 - (c) *if there are any degree 3 nodes on the boundary, all of the degree 2 nodes cannot be consecutive; and*
 - (d) *if the degree 2 nodes on both ends of a chain of degree 3 boundary nodes are removed, the graph remains connected.*

Proof: Let G be a filled triangulation graph. Since it is biconnected, it cannot have any vertices of degree 1. Its triangulation representation yields an embedding with all internal nodes of degree 3. Lemma 1 shows we have at least 3 nodes of degree 2 on the boundary.

Suppose there are degree 3 nodes on the boundary and the degree 2 nodes are consecutive. The chain of degree 2 nodes cannot connect at a single vertex, because this would be a cut vertex. Thus, if we remove all triangles corresponding to degree 2 nodes, we would have a triangulation representation of a graph with exactly 2 vertices of degree two, which is not allowed by Lemma 1.

To finish the proof of necessity, we note that for two degree 2 triangles to disconnect the triangulation, they would have to share an interior vertex. On the other hand, if all intervening triangles on the boundary have degree 3, they can contribute nothing to the polygon boundary, so the two degree 2 must share another vertex. But then, they share a side, so there can't be any intervening degree 3 triangles.

Next, we prove sufficiency. We assume G is biconnected, all of its vertices have degree 2 or 3, and it has the specified embedding. We construct a graph G' which is a special kind of dual of G . G' contains the dual of the interior faces and edges of G . In addition, G' has a vertex for each maximal sequence of degree 3 nodes on the boundary, and a vertex for each boundary edge connecting two degree 2 nodes. These are placed in the external face of G , near the corresponding nodes or edges. These vertices are connected in a cycle of G' following the ordering induced by the boundary nodes and edges of G . Finally, for each boundary edge e of G , we add an edge from the node of G' corresponding to the interior face of G containing e to one of the vertices on the external cycle of G' . If e is adjacent to a vertex of degree 3, we connect the edge to the node of G' corresponding to the degree 3 vertex. Otherwise, we connect to the node of G' corresponding to e .

It is immediate from the construction that G' is a planar embedding of nodes and edges; all interior faces are triangles; and there is a 1-1 correspondence between faces of G' and vertices of G and between edges in G and G' . We need to show that G' is a simple graph.

As G is biconnected, G' can have no loops. Property 2(d) of the embedding implies that each interior face is connected to at most one of the nodes associated with the exterior face. The only way that multiedges could then occur would be if G' has a boundary consisting of two nodes and two edges. We know G has at least $n_2 \geq 3$ nodes of degree 2 on the boundary. If there are only degree 2 nodes on the boundary, G' has a boundary of n_2 nodes. Assume G has some degree 3 nodes on the boundary. If these nodes split into 3 or more paths, the construction creates at

least 3 nodes on the boundary of G' . If not, they must split into 2 paths, since the degree 2 nodes must be separated. One group of degree 2 nodes must contain at least 2 nodes. The construction then creates one node for each group of degree 3 nodes, and at least one node for the path of more than 2 degree nodes, again given G' at least 3 boundary nodes.

As G' is simple, by using one of the algorithms (e.g, [8]) for making the edges of planar graph into line segments while retaining the embedding, we derive a triangulation representation of G , completing the proof. \square

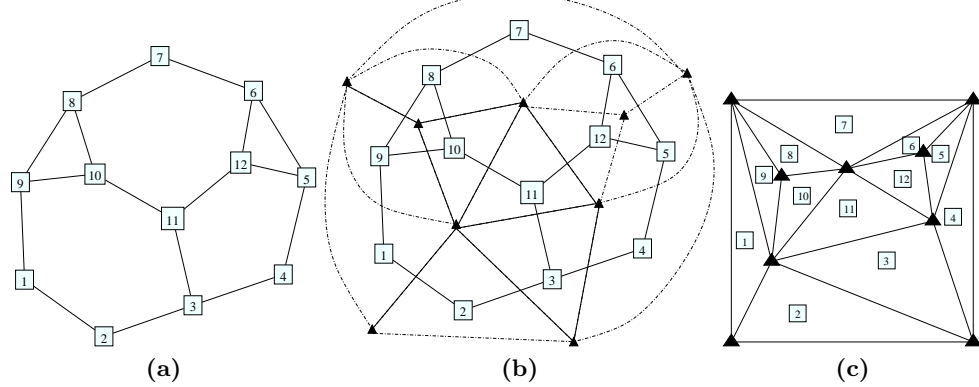


Fig. 3. Constructing a triangulation graph. (a) Original graph; (b) Creating the “dual” graph; (c) Straightening the edges.

Perhaps not surprisingly, the conditions of the theorem have a similar feel to those for rectangular drawings [17]. It is also not hard to see that the result can probably be derived from the duality between planar, cubic, 3-connected graphs and triangulations of the plane [18], but our proof seems more straightforward. Lastly, we note that Theorem 3 gives another proof that the hexagonal grid graphs of Section 3 have a touching triangle representation.

Figure 3 demonstrates the algorithm. Figure 3(a) shows a graph satisfying the conditions of the theorem. In Figure 3(b), we have added a node for each internal face, and node on the outside for each sequence of degree 3 nodes or for each edge both of whose nodes have degree 2. This gives us a planar graph with each face having three sides and associated with a node of the original graph. Straightening the sides of the faces makes each face a triangle.

5 Necessary conditions

Thus far, we have shown that various categories of graphs are in TTG . Now, we wish to pursue some necessary conditions which will eliminate many graphs from TTG . We start with some definitions.

Given triangles T_0 and T_1 , pick two sides s_0 and s_1 , one from each triangle, and orient the side counter-clockwise around the interior of the triangle. Extend the sides into directed lines L_0 and L_1 . If the lines intersect at a unique point, the intersection is *feasible* if a non-trivial portion of s_0 lies to the right of L_1 and a non-trivial portion of s_1 lies to the right of L_0 . Of the four angles formed at a feasible intersection, there is a unique one corresponding to a right turn. We call this a *feasible angle*. Two sides are *collinear* if the directed lines L_0 and L_1 are identical.

Lemma 2. *If a triangle T touches both T_0 and T_1 , using two distinct sides, one of its angles must be a feasible angle of T_0 and T_1 .*

Proof: If α is the angle of T determined by the two touching sides of T_0 and T_1 , it immediate that α is a feasible angle. See Figure 4. \square

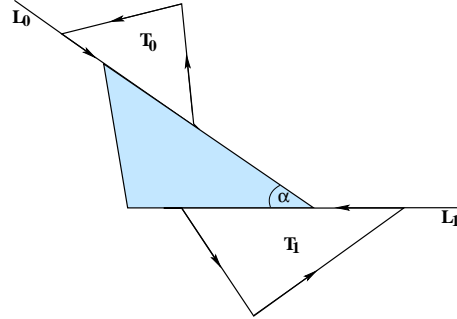


Fig. 4. A triangle T touching two other triangles T_0 and T_1 . The angle α is a feasible angle of T_0 and T_1 .

This lemma already greatly reduces the possible TTG graphs. If two triangles have no collinear sides, there can be at most nine triangles touching both both of them, since any such triangle eliminates at least one of the feasible angles. If two sides are collinear, one triangle can touch those two sides. Any other triangles must correspond to feasible angles, and since the remaining sides of both triangles are all to the left of the two collinear sides, there can be at most 4 feasible angles. We next work at tightening these bounds.

For a node u in G , we let N_u be the nodes in G joined to u by an edge. If u and v are two nodes in a graph G , define N_{uv} as the mutual neighbors of u and v , that is, $N_{uv} = N_u \cap N_v$. Finally, define E_{uv} be the subset of edges of G induced by N_{uv} .

Theorem 4. Let G be a TTG , and let u and v be two nodes in G joined by an edge. Then $|N_{uv}| \leq 3$ and $|E_{uv}| \leq 1$.

Proof: Let T_u and T_v be the two triangles corresponding to nodes u and v . Since the two nodes share an edge, T_u and T_v must touch. There are basically two possibilities: one side is totally contained in the other or not.

In the first case, we have the situation represented in Figure 5. We immediately note that there can be no feasible angle associated with $\vec{12}$ and \vec{ab} . In addition, \vec{ab} is to the left of both $\vec{23}$ and $\vec{31}$. On the other hand, there are feasible angles formed by $\vec{12}$ with \vec{bc} and \vec{ca} . So, we only have to consider pairings of $\vec{23}$ and $\vec{31}$ with \vec{bc} and \vec{ca} .

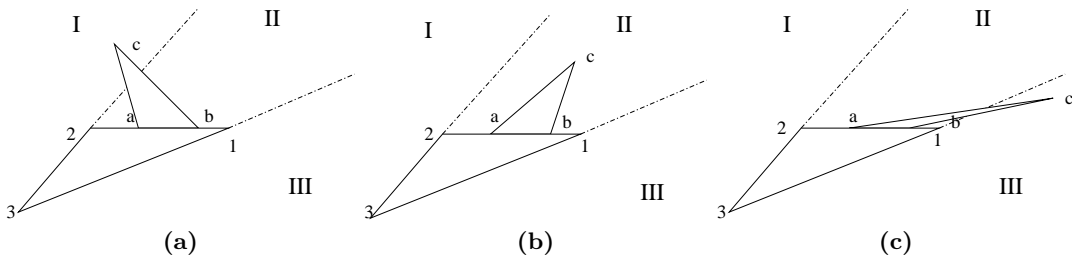


Fig. 5. Touching triangles with one side contained in the other. (a) Node c in region I; (b) Node c in region II; (c) Node c in region III.

If point c is placed in region II, both \vec{bc} and \vec{ca} are to the left of $\vec{23}$ and $\vec{31}$, so there are no more feasible angles, giving a total of two.

If c is in region III, we get a new feasible angle formed by $\vec{31}$ and \vec{bc} . In this case, though, we are left with \vec{bc} and \vec{ca} to the left of $\vec{23}$, and $\vec{31}$ to the left of \vec{ca} . Thus, we have at most three feasible points. We also note that any triangle associated with the feasible angle formed by $\vec{12}$ and \vec{ca} cannot share an edge with any triangle of the other two feasible angles, so there can be at most one edge among the neighbors of u and v .

The argument is similar if c is in region I.

If points 1 and b are identical, the same arguments hold except, in addition, we no longer have a feasible angle formed by $\vec{12}$ and \vec{bc} because $\vec{12}$ is to the left of \vec{bc} . Thus, we have at most two mutual neighbors and no edge between them. If points 2 and a are the same, the same arguments hold. Putting these two cases together, we find that if 1 and b are identical and 2 and a are identical, there can be at most one feasible angle.

The remaining case occurs when neither shared side is contained in the other. This is the situation represented by Figure 6.

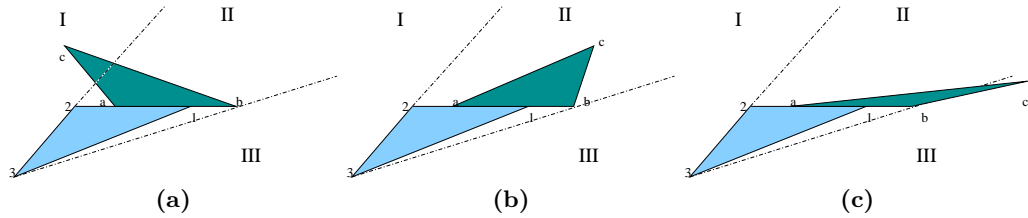


Fig. 6. Touching triangles with touching sides overlapping. (a) Node c in region I; (b) Node c in region II; (c) Node c in region III.

As previously, there can be no feasible angle associated with $\vec{12}$ and \vec{ab} , but now we have feasible angles formed by $\vec{12}$ and \vec{ca} , and by $\vec{31}$ and \vec{ab} . In addition, $\vec{12}$ is to the left of \vec{bc} and \vec{ab} is to the left of $\vec{23}$. Again, we are reduced to considering the four pairings of $\vec{23}$ and $\vec{31}$ with \vec{bc} and \vec{ca} . If \vec{ca} is to the right of $\vec{31}$, then $\vec{31}$ is to the left of \vec{ca} , and vice versa, so that pairing is not possible. Finally, we note that if c is in regions I or II, then $\vec{23}$ and $\vec{31}$ are to the left of \vec{bc} , while if c is in regions II or III, \vec{bc} and \vec{ca} are to the left of $\vec{23}$. So, if c is in region II, there are at most two feasible angles. Otherwise, there can be three but, as above, at most two of the associated triangles can touch. \square

With this theorem, we see that the left two graphs in the top row of Figure 10 are not in TTG . We next consider what happens to the set of common neighbors if we relax the condition that there is an edge between two nodes.

Theorem 5. *Let G be a TTG , and let u and v be any two nodes in G . Then $|N_{uv}| \leq 4$ and $|E_{uv}| \leq 2$.*

Proof: The proof follows that style of the previous theorem. Let T_u and T_v be the two triangles corresponding to nodes u and v . We have already dealt with the two triangles sharing a side above. So, we then consider the case when a pair of sides are collinear, as illustrated in Figure 7.

For this case, we can place a triangle touching $\vec{12}$ and \vec{ab} . Since both triangles are to the left of both $\vec{12}$ and \vec{ab} , these sides cannot be used in any other feasible angle. There can be no feasible angle formed by $\vec{23}$ and \vec{ca} , since, if any part of \vec{ca} is to the right of $\vec{23}$, the latter must be to the left of \vec{ca} , and vice versa. In addition, there can only be one of the two possible feasible angles

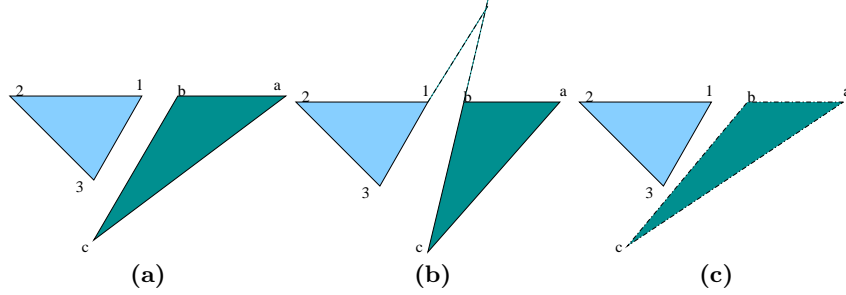


Fig. 7. Collinear sides (a) $\vec{31}$ and \vec{bc} parallel; (b) $\vec{31}$ and \vec{bc} meeting above; (c) $\vec{31}$ and \vec{bc} meeting below.

formed by $\vec{23}$ and \vec{bc} or by $\vec{31}$ and \vec{ca} . Thus, there can be at most three touching triangles. (A more careful analysis shows that case (a) can have at most two, while cases (b) and (c) will have three only if the triangles touch.)

For the next case, we consider when a vertex of one triangle touches the interior of a side of the other, as shown in Figure 8. The dotted lines indicate the lines $\vec{23}$ and $\vec{31}$, and divide the area into three regions. We consider the cases determined by which regions contain vertices a and b . We note that if a is in region I, b must also be in that region. We can also assume that both a and b do not lie on either $\vec{23}$ and $\vec{31}$, as this was covered by the collinear case addressed above. In all cases, we have feasible points determined by $\vec{12}$ with both \vec{ca} and \vec{bc} . Also, in all cases either \vec{ca} is to the left of $\vec{23}$, or vice versa, so this pair is eliminated. The similar condition holds for \vec{bc} and $\vec{31}$.

For the case when \vec{ab} lies in region II (Figure 8(a)), $\vec{12}$ can also form a feasible point with \vec{ab} . On the other hand, the triangle abc lies to the left of both $\vec{23}$ and $\vec{31}$, so we are limited to three feasible points.

When \vec{ab} lies in region I (Figure 8(b)), the triangle abc is to the left of $\vec{31}$, so the latter has no feasible points. There is always a feasible point fixed by $\vec{23}$ and \vec{bc} . If $\vec{12}$ is to the left of \vec{ab} , the only remaining possibility is given by \vec{ab} and $\vec{23}$. If $\vec{12}$ is partly to the right of \vec{ab} , both \vec{ab} and $\vec{23}$ and \vec{ab} and $\vec{12}$ give feasible points, but a triangle placed at one blocks the other (and the feasible point of $\vec{23}$ and \vec{bc} as well). Thus, we are limited to four touching triangles.

The case when \vec{ab} lies in region III (Figure 8(c)) is symmetric.

We next consider b in region I and a in region II (Figure 8(d)). The triangle abc is to the left of $\vec{31}$, so the latter has no feasible points. In addition, $\vec{23}$ is to the left of \vec{ab} , leaving at most four feasible points.

If we leave a in region II but move b to region III (Figure 8(e)), we have a similar situation, with triangle abc is to the left of $\vec{23}$ and \vec{ca} is to the left of $\vec{31}$.

Switching their roles, with a in region III and b in region II (Figure 8(f)), we still have triangle abc is to the left of $\vec{23}$ but now $\vec{31}$ is to the left of \vec{ab} .

In the final sub-case, b lies in region I and a lies in region III (Figure 8(g)). Here, the triangle 123 lies to the left of \vec{ab} , eliminating all feasible points involving the latter. We are left with two remaining possibilities: \vec{bc} with $\vec{23}$ and \vec{ca} with $\vec{31}$, for a total of four.

Next, we assume the triangles touch at two vertices, as shown in Figure 9. There can be a feasible point formed by $\vec{23}$ and \vec{ca} , and one by $\vec{31}$ and \vec{bc} . On the other hand, we can immediately eliminate the pairs $\vec{23}$ and \vec{bc} , and $\vec{31}$ and \vec{ca} . If \vec{ab} is in the left half plane of $\vec{12}$ (Figure 9(a)), the latter has no feasible points. Thus, there can be at most four. In fact, \vec{ab} can have at most one feasible point, with either $\vec{31}$ or $\vec{23}$, but not both, so there are at most 3 feasible points.

Otherwise, either point a or point b is to the right of $\vec{12}$ (Figure 9(b)), all of triangle 123 is to the left of \vec{ab} , and the symmetric case holds, with no feasible points associated with \vec{ab} , and at most one additional feasible point formed by $\vec{12}$ and either \vec{ca} or \vec{bc} .

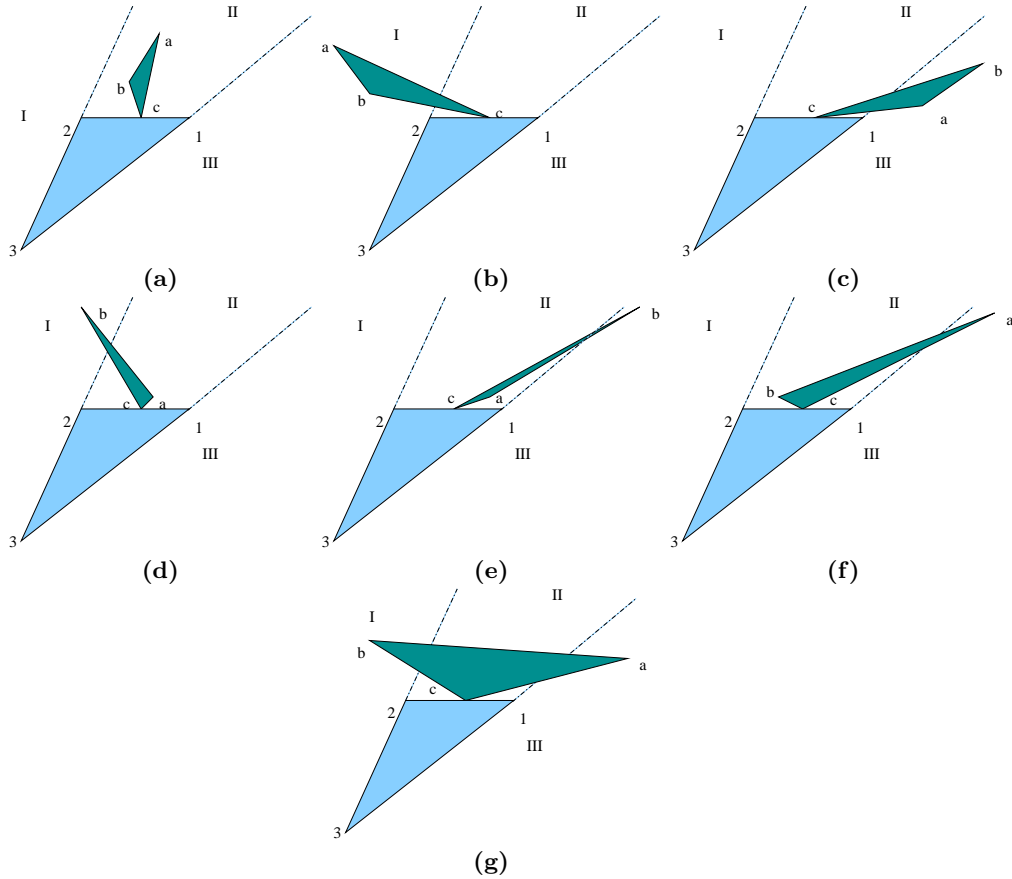


Fig. 8. Triangles touch at vertex and side. (a) \vec{ab} to region II; (b) \vec{ab} in region I; (c) \vec{ab} in region III; (d) b in region I, a in region II; (e) b in region III, a in region II; (f) b in region II, a in region III; (g) b in region I, a in region III.

Finally, if the triangles do not touch at all and do not have a pair of collinear sides, consider a pair of closest points p_0 and p_1 , one on each triangle, and the line segment between the two points. If we imagine translating the points along this line segment until the triangles touch, we have one of the three situations: that of Theorem 4, Figure 8 or Figure 9, and similar analysis apply, but with a possible reduction in usable feasible points. For example, consider the configuration of Figure 8(c).

This fits the pattern of Figure 9(a). Thus, $\vec{12}$ has no feasible points, and \vec{ab} might potentially form a feasible point with $\vec{23}$ or $\vec{31}$, but not both. Now, unlike the touching case, we have four feasible points from sides $\vec{23}$, $\vec{31}$, \vec{bc} and \vec{ca} . The problem is that, if a triangle is placed at one of those points, the remainder become unusable. Thus, we end up with at most three neighboring triangles. To complete the proof, we note that, in all of the cases, there can be at most two pairs of touching triangles among the ones added. \square

Figures 8 and 9 show that the bounds of 3 or 4 derived in the proof are tight. Theorem 5 shows that the top right graph in Figure 10 is not TTG. Although these two theorems provide simple tests for eliminating potential TTGs, we are fairly certain that they do not provide sufficient conditions.

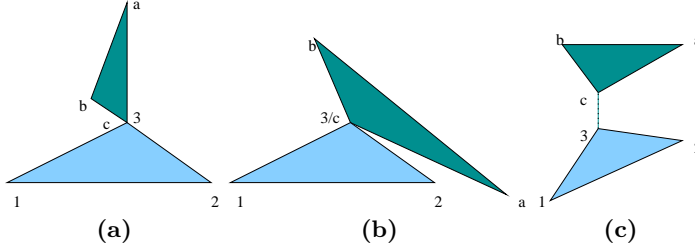


Fig. 9. Triangles touch at two vertices (a) \vec{ab} to the left of $\vec{12}$; (b) \vec{ab} crossing $\vec{12}$; (c) shows one case of non-touching triangles.

6 Conclusion and Future Work

We have considered the class of graphs that can be represented as contact graphs of triangles, and shown that this includes outerplanar graphs as well as subgraphs of square and hexagonal grids. We derived some necessary conditions for such graphs, and was able to present a complete characterization of the special subclass of biconnected triangulation graphs. A complete characterization of TTG , as well as contact graphs of 4-gons and 5-gons, remains open.

References

1. M. Bern. Triangulations. In J. E. Goodman and J. O'Rourke, editors, *Handbook of Discrete and Computational Geometry*, CRC Press, 1997. 1997.
2. G. R. Brightwell and E. R. Scheinerman. Representations of planar graphs. *SIAM Journal on Discrete Mathematics*, 6(2):214–229, May 1993.
3. A. L. Buchsbaum, E. R. Gansner, C. M. Procopiuc, and S. Venkatasubramanian. Rectangular layouts and contact graphs. *ACM Transactions on Algorithms*, 4(1), 2008.
4. M. de Berg, E. Mumford, and B. Speckmann. On rectilinear duals for vertex-weighted plane graphs. *Discrete Mathematics*, 309(7):1794–1812, 2009.
5. M. de Berg, M. van Kreveld, M. H. Overmars, and O. Schwarzkopf. *Computational Geometry: Algorithms and Applications*. Springer-Verlag, 2nd edition, 2000.
6. H. de Fraysseix, P. O. de Mendez, and P. Rosenstiehl. On triangle contact graphs. *Combinatorics, Probability and Computing*, 3:233–246, 1994.
7. H. de Fraysseix, P. O. de Mendez, and P. Rosenstiehl. Representation of planar hypergraphs by contacts of triangles. In *15th Symposium on Graph Drawing*, pages 125–136, 2007.
8. H. de Fraysseix, J. Pach, and R. Pollack. Small sets supporting Fary embeddings of planar graphs. In *Proc. 20th Symposium on Theory of Computing (STOC)*, pages 426–433, 1988.
9. C. A. Duncan, E. R. Gansner, Y. Hu, M. Kaufmann, and S. G. Kobourov. Optimal polygonal representation of planar graphs. 2009. preprint.
10. F. Harary. *Graph Theory*. Addison-Wesley, Reading, MA, 1972.
11. X. He. On finding the rectangular duals of planar triangular graphs. *SIAM Journal of Computing*, 22(6):1218–1226, 1993.
12. X. He. On floor-plan of plane graphs. *SIAM Journal of Computing*, 28(6):2150–2167, 1999.
13. J. Hopcroft and R. E. Tarjan. Efficient planarity testing. *Journal of the ACM*, 21(4):549–568, 1974.
14. G. Kant. Hexagonal grid drawings. In *18th Workshop on Graph-Theoretic Concepts in Computer Science*, pages 263–276, 1992.
15. P. Koebe. Kontaktprobleme der konformen Abbildung. *Berichte über die Verhandlungen der Sächsischen Akademie der Wissenschaften zu Leipzig. Math.-Phys. Klasse*, 88:141–164, 1936.
16. C.-C. Liao, H.-I. Lu, and H.-C. Yen. Compact floor-planning via orderly spanning trees. *Journal of Algorithms*, 48:441–451, 2003.
17. M. Rahman, T. Nishizeki, and S. Ghosh. Rectangular drawings of planar graphs. *Journal of Algorithms*, 50(1):62–78, 2004.
18. E. Steinitz and H. Rademacher. *Vorlesungen über die Theorie der Polyeder*. Springer-Verlag, Berlin, 1934.
19. C. Thomassen. Plane representations of graphs. In J. A. Bondy and U. S. R. Murty, editors, *Progress in Graph Theory*, pages 43–69. Academic Press, Canada, 1984.

Appendix: Non-TTG Planar Graphs

Here we briefly illustrate that the property “representable as TTG” is not closed under homeomorphisms or minors. Specifically, the graphs in Figure 10 cannot be represented as TTGs, but subdividing one edge from each of them makes them representable as TTGs.

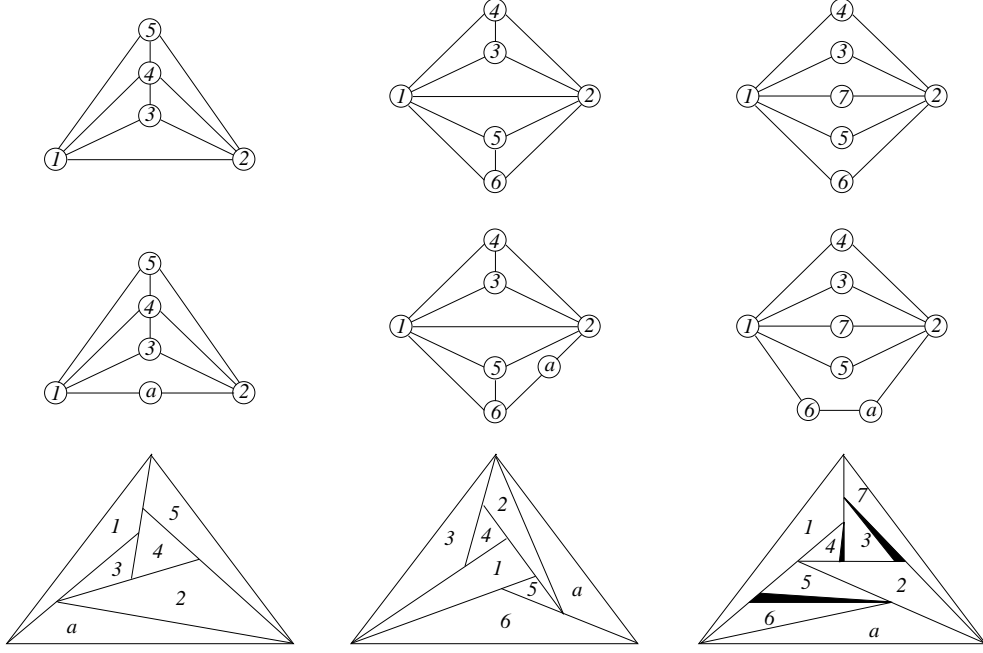


Fig. 10. The graphs in the first row (on 5, 6, 7 vertices) do not have touching triangle graph representations. However, subdividing one edge from each, as in the second row, results in graphs that have TTG representations. These representations are shown in the third row.